Optical Telemetry Ranging

Marc Sanchez Net* and Jon Hamkins†

ABSTRACT. — Optical Telemetry Ranging is a ranging scheme conceived for space-to-ground links operating at optical frequencies. Its underlying principle is inherited from Radio Frequency (RF) Telemetry Ranging — generalized phase measurements required to estimate the two-way light-time delay are acquired on board the spacecraft and then telemetered back to Earth. However, and unlike the RF Telemetry Ranging, no dedicated uplink ranging signal is required for the system to operate. Instead, the uplink frame structure is used to define and measure the uplink signal phase.

This article describes how Optical Telemetry Ranging can be implemented in current space optical communication systems. To that end, it first describes the concept of operation assuming an idealized link and measurement system where all signals are continuous and can be sampled instantaneously. Then, it explains how the system can be adapted to work within the design of discrete-time optical transmitters and receivers currently under development. Finally, we discuss how to encode phase measurements taken on board the spacecraft and show that the bandwidth overhead incurred in the downlink is, in most cases, negligible.

I. Introduction

Ranging is an integral data product for space navigation. It provides accurate measurements of distance between a spacecraft and an Earth station by measuring the two-way time delay of a signal traveling between both assets. These ranging measurements, together with other navigation data products (e.g., Doppler shift and Doppler rate, antenna tracking angles), are then used for orbit determination and propagation, which in turn, informs mission planning.

---

*Communications Architectures and Research Section.

†Communications, Tracking and Radar Division.

The research described in this publication was carried out by the Jet Propulsion Laboratory, California Institute of Technology, under a contract with the National Aeronautics and Space Administration.

Several ranging methods are currently used and/or standardized for missions communicating with Earth via RF signals. These include sequential ranging [1], pseudo-noise (PN) Ranging [2, 3], combined Gaussian minimum-shift keying (GMSK) and PN ranging [4], and telemetry ranging [5]. Some methods, most notably sequential ranging, have widespread adoption among current deep space missions, while others have only been chosen to a lesser extent. For instance, New Horizons was the first mission to use PN ranging. Some methods have not flown operationally to date.

Ranging for missions establishing links using optical communications (also known as optimetrics) has been studied in the literature (e.g., [6]). In fact, the Lunar Laser Communication Demonstration (LLCD) experiment supported the ability to obtain ranging measurements while transmitting Pulse Position Modulation (PPM) symbols with a noise floor of less than 1 cm [7]. This was achieved by having the spacecraft uplink and downlink clocks synchronized, and timing the departures of downlink frames to arrivals of uplink frames.

In this article, we focus our attention on optometric ranging. We impose little restrictions on the overall system architecture, except that ranging measurements must be performed between an Earth optical aperture and a spacecraft without intermediate space-based relays. Furthermore, since space optical communication systems through the atmosphere typically use non-coherent modulation schemes, we also assume that optimetric techniques relying on carrier phase measurements are not in scope, despite acknowledging that theoretically, significant ranging precision improvements are possible in that regime [6].

II. Ranging Preliminaries

We consider the end-to-end ranging system between an Earth telescope, nominally a deep space station (DSS), part of the Deep Space Network (DSN), and a spacecraft. The uplink (the link from the ground telescope to the spacecraft) can be established using optical or RF communications. On the other hand, the downlink (the link from the spacecraft to the ground telescope) is always assumed to operate at optical frequencies.

Figure 1 shows the different elements[1] relevant for implementing a ranging system along with the delays incurred at different stages of the transmission path. The ground station signal processing center (SPC) has a common ultra-precise (1 ns accuracy) 1 pulse-per-second (1-PPS) clock reference that can be shared between the uplink and downlink digital signal processing (DSP) equipment. In contrast, we assume that the spacecraft has two internal clocks that need not be synchronized, one for uplink and another for downlink.

[1]Figure 1 depicts two optical apertures — one for transmitting and one for receiving. However, they typically refer to the same physical DSS.

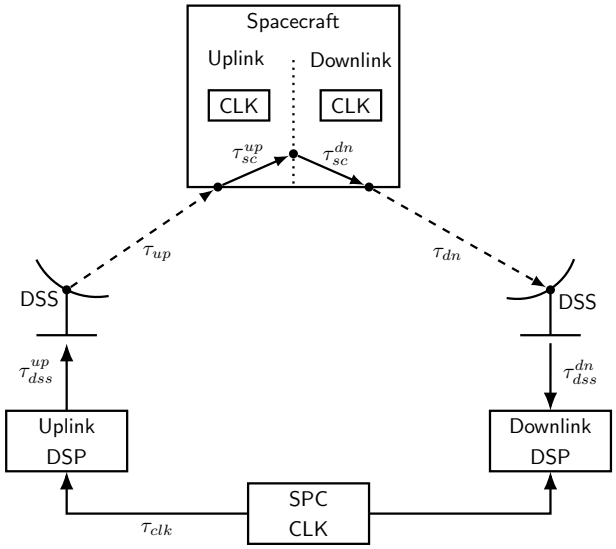

Figure 1. End-to-end Ranging System

The primary goal of the ranging system is to estimate the two-way delay $\tau_{up} + \tau_{dn}$ between the ground station and the spacecraft. Traditionally, this has been accomplished by measuring the phase difference between the transmitted and received signals, which are assumed to be periodic. Then, the two-way light-time delay can be estimated as a function of this phase difference, and a set of constant delay contributions τ_{dss}^{up}, τ_{sc}^{up}, τ_{dss}^{dn}, τ_{sc}^{dn} that must be calibrated prior to performing the range measurements and that we lump into single value.[2]

$$\tau_{cal} = \tau_{dss}^{up} + \tau_{sc}^{up} + \tau_{dss}^{dn} + \tau_{sc}^{dn} \tag{1}$$

A. General Definition of Phase

Let $r(t)$ be a periodic signal of period T. Then, it is common practice to define its phase as

$$\phi(t) = 2\pi \frac{t - t_0}{T} \mod 2\pi, \; t \geq t_0, \tag{2}$$

where t_0 is an arbitrary initial instant in time that is associated with the beginning of a cycle. For the purposes of this paper, however, let us consider a normalized and unwrapped phase definition

$$\varphi(t) = \text{unwrap}\left(\frac{\phi(t)}{2\pi}\right) = \frac{t - t_0}{T}, \tag{3}$$

where $\varphi(t) \in \mathbb{R}^+$ is simply a monotonically increasing number that indicates how many cycles have elapsed since the arbitrary origin. Finally, let us decompose $\varphi(t)$ in

[2]Ground station delays are generally calibrated before each ranging pass as they might vary over time. In contrast, delays on the spacecraft are typically calibrated prior to launch and assumed to be constant for the rest of the mission.

its integer and fractional part,

$$\varphi(t) = s(t) + \epsilon(t), \tag{4}$$

where $s(t) \in \mathbb{N}$ changes once every T seconds, and $\epsilon(t) \in [0, 1)$ varies constantly.

Figure 2 shows $\varphi(t)$ for three notional periodic signals. On the left column, the presented signal is just a sine wave of constant frequency, which could be equal, for instance, to a carrier or subcarrier tone. On the center column, the signal is a bit stream pattern with 3-bit periodicity, which could be obtained by transmitting a PN sequence. Finally, the right-hand column shows a periodic signal in which information from the frame structure (e.g., synchronous markers) is periodically detected to delimit the beginning and end of any given cycle.

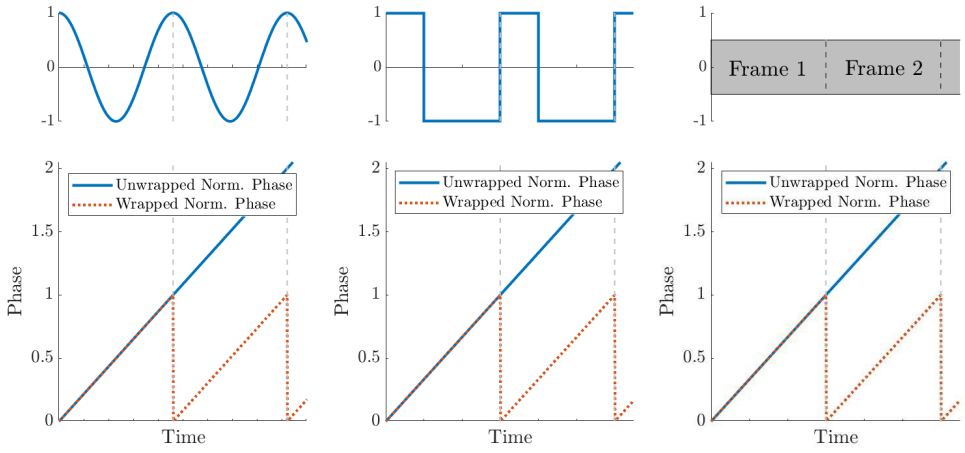

Figure 2. Phase Definition

B. Range Ambiguity and Range Resolution

Ranging systems have two primary requirements: range ambiguity (RA) and range resolution (RR). The RA indicates the minimum distance for which ranges d, $2 \cdot d$, $3 \cdot d$, etc., cannot be distinguished from one another by the ranging system. In particular, in order to derive a range measurement from a periodic signal sent to and returned by a spacecraft, less than a full cycle must elapse between the departure and arrival times. Therefore, and given that electromagnetic waves propagate at a constant speed c in the vacuum, we obtain that $\tau_{up} + \tau_{dn} = \frac{2d}{c}$ must be less than T and, consequently,

$$d_{RA} = \frac{c \cdot T}{2}. \tag{5}$$

This explains, for instance, why ranging cannot be performed with a single tone at the carrier frequency. Indeed, at $f_c = 2$ GHz (S-band), any spacecraft motion exceeding 7.5 cm over a round-trip light time would not be properly disambiguated.

On the other hand, the RR refers to the range precision achievable by the ranging system and is dictated by the ability of our measurement instruments to accurately track and monitor the phase of the transmitted and received signals over time. There are several technical limitations that can affect this value: spacecraft oscillator frequency instability, maximum instrument sampling rate, analog-to-digital converter timing jitter, group delay effects in transmission lines caused by temperature changes, etc. Ultimately, however, most ranging systems for deep space communications are limited by noise, which corrupts the received signal and induces variance on the carrier and timing tracking loops at the receiver.

III. Optical Telemetry Ranging

Optical Telemetry Ranging (OTR) adapts the ranging philosophy of RF Telemetry Ranging [8, 9, 10] to spacecraft carrying an optical telescope. In particular, the measurement is conducted on board the spacecraft using its uplink and downlink subsystems, and then telemetered back to Earth as part of the normal telemetry stream. This contrasts with conventional ranging, where all measurements are conducted at the ground station and the spacecraft simply acts as a "mirror" that transfers timing information between the spacecraft's uplink and the downlink subsystem.

There are several advantages to using OTR over conventional ranging methods. Some advantages are inherited from the strengths of RF telemetry ranging. For instance, high-rate telemetry and ranging measurements can be performed simultaneously during the entire pass. Similarly, no power is dedicated to the ranging signal on the downlink, a consideration especially beneficial for deep space missions. Compared to conventional optical ranging approaches such as Time of Flight (ToF) [7], which requires the spacecraft to synchronize the uplink and downlink clocks, OTR imposes no timing restriction. Whereas ToF requires an optical uplink beacon carrying valid codewords,[3] OTR can work with an uplink signal that is either RF or optical, and can carry frames, codewords, or even a PN sequence.

In Section III.A we describe the concept of Optical Telemetry Ranging assuming an idealized time system where all signals are continuous in time and phase measurements can be taken at any point in time instantaneously. In Section III.B, we explain how the OTR system can be implemented in discrete-time. Lastly, in Section III.C, we detail how the OTR measurements should be encoded as part of the telemetry stream from the spacecraft to Earth.

---

[3]These codewords might contain fill bits. What really matters is that the frame structure can be detected via synchronization markers.

A. OTR Concept

Figure 3 provides a schematic diagram of the uplink and downlink signals involved in an OTR system. The ground station sends a stream of uplink frames to the spacecraft with an identifier that increases from 0 to $N_u - 1$, and then starts back at one. At the same time, and in a completely asynchronous fashion, the spacecraft sends a stream of downlink frames to the ground, with their own identifier ranging from 0 to $N_d - 1$.

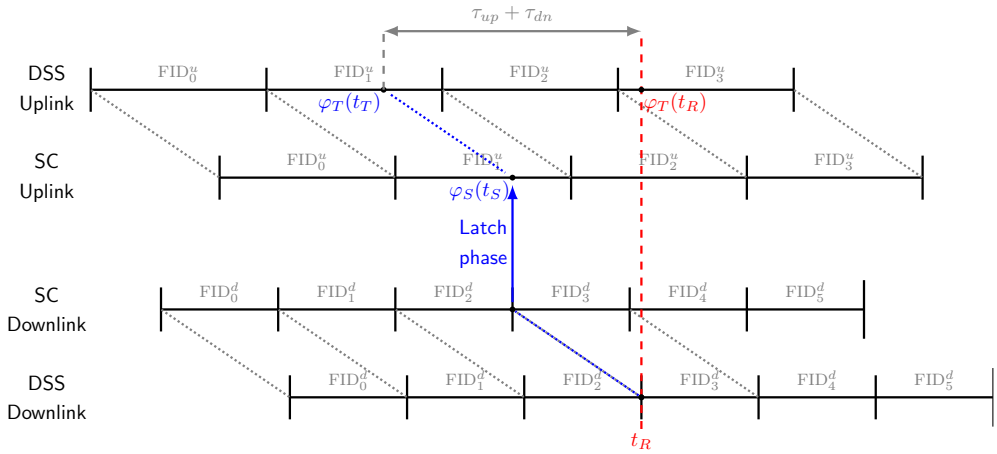

Figure 3. OTR Concept

The ranging subsystem on the ground station acquires an estimate of the propagation delay between the spacecraft and the ground station every time a downlink frame starts arriving, an event henceforth denoted by t_R (see red dashed line in Figure 3). To do so, it must first estimate the two-way propagation delay between the spacecraft and the ground station

$$\tau(t_R) = (t_R - t_T) - \tau_{cal}, \tag{6}$$

and then recover a range estimate by solving

$$\tau(t_R) = \frac{2d(t_R)}{c}, \tag{7}$$

where c is the speed of light in the vacuum.[4] Therefore, the range estimation problem is equivalent to estimating the two-way light-time delay between the spacecraft and the ground station.

Assuming that τ_{cal} is known a priori, the only unknown left in Equation (6) is t_T. To infer it, we need to estimate the instant of time in which $\varphi_T(t_T)$ appeared at the ground station's uplink subsystem, a value that can be computed by converting

[4]Delays due to speed of light differences while traversing the atmosphere could be incorporated by having a more general expression relating τ and d. However, they are left outside of the scope of this article.

phase-delay measurements of the uplink transmitted signal to time-delay measurements [8, 11]:

$$\int_{t_T}^{t_x} \dot{\varphi}_T(t)dt = \varphi_T(t_x) - \varphi_T(t_T). \tag{8}$$

In Equation (8), $\dot{\varphi}_T(t)$ denotes the time derivative of phase of the transmitted signal by the ground station, a value that can be measured and stored at any point in time; $\varphi_T(t_x)$ is the phase of the uplink signal at t_x, an arbitrary point in time that is used as a reference; and $\varphi_T(t_T)$ is the phase of the transmitted signal at $t_T = t_R - \tau(t_R)$. Note that if $\varphi_T(t_T)$ is known, then Equation (8) has only one unknown, t_T, and therefore can be solved directly. This, in turn, allows us to solve Equation (6) and finally use Equation (7) to recover a range estimate.

For this procedure to work, it is clearly necessary to have an estimate of $\varphi_T(t_T)$. Figure 3 shows how this is achieved in OTR. In particular, assume that the ranging measurement is to be taken at time t_R. This same event will have occurred on board the spacecraft τ_{dn} seconds earlier when the same frame was departing. Therefore, a phase measurement on board the spacecraft at that time $t_S = t_R - \tau_{dn}$ can be associated with time t_R on the ground.

Let us now assume that at time t_S the spacecraft measures a phase $\varphi_S(t_S)$ on its received uplink stream.[5] Then, this phase will have occurred τ_{up} seconds earlier in the ground station's uplink transmitter. Therefore, we have devised a system in which

$$\varphi_T(t_T) = \varphi_S(t_S). \tag{9}$$

In other words, the phase telemetered from the spacecraft to the ground can be directly compared at time t_R with the phase measured on the ground station's uplink subsystem.

1. Range Estimation for a Link without Doppler Shifts

To demonstrate how a range measurement would be obtained in a simplistic setup, let us first consider an ideal link where the optical carrier experiences no Doppler shift. In that case,

$$\dot{\varphi}_T(t) = \frac{d}{dt}\varphi_T(t) = \frac{d}{dt}\frac{t - t_0}{T} = \frac{1}{T} \tag{10}$$

and, consequently, Equation (8) simplifies to

$$\frac{t_R - t_T}{T} = \varphi_T(t_R) - \varphi_T(t_T). \tag{11}$$

---

[5]The time t_S need not be explicitly known for the ranging system to work. However, it is included to adequately explain the timing of events on Figure 3.

Combining this result with Equations (6) and (9) yields the following closed-form solution for the range estimate:

$$\hat{d}(t_R) = \frac{c \cdot T}{2} \left[\varphi_T(t_R) - \varphi_S(t_S)\right]. \tag{12}$$

Also, if a calibration delay needs to be corrected during the range computation, then

$$\hat{d}(t_R) = \frac{c}{2} \left[T \left[\varphi_T(t_R) - \varphi_S(t_S)\right] - \tau_{cal}\right]. \tag{13}$$

2. Range Estimation for a Link with Doppler

In traditional Deep Space Network operations, the RF uplink signal sent by the ground station is usually Doppler pre-compensated. This ensures that the spacecraft radio can acquire the uplink carrier, track it, and start the demodulation process. This same argument is also valid for optical communications, except that in this case, the wavelength of the modulating laser is shifted according to predictions of the Doppler effect from spacecraft trajectory estimates.

The primary effect of having a non-zero Doppler shift in the link is that $\dot{\varphi}_T(t)$ is no longer constant and equal to $\frac{1}{T}$. This, in fact, indicates that the net effect of a Doppler shift is to lengthen and/or shorten the duration of bits, symbols, and frames, which we had assumed constant in Figure 3. Therefore, when computing ranging estimates, Equation (8) will no longer have a closed form solution and, instead, t_T will have to be derived numerically from the available measurements. Evidently, this changes the mechanics of the ranging determination procedure, but the basic underlying principles remain unchanged.

B. OTR Phase Measurements

Section III.A explains the concept of Optical Telemetry Ranging assuming an ideal system where all signals are continuous in time. In reality, however, both the transmitter and receiver of the ground station and the spacecraft will have discrete-time electronics that operate on a sample-by-sample basis. Therefore, this section details the exact measurements taken by each part of the system and explains how to deal with phase offsets that result from the time-discretization process.

Figure 4 shows the different discrete-time measurements taken by the ground station. On the uplink side, two data sets are recorded: one for the phase of the transmitted signal and another one for its derivative. We also assume that both of them are triggered by the same mechanism, nominally a 1-PPS ultra-stable clock reference. Therefore, we denote the resulting discrete-time series by

$$\varphi_T[t_P] = \left\{t_{P_0} : \varphi_{T_0}, t_{P_1} : \varphi_{T_1}, ..., t_{P_{K_P-1}} : \varphi_{T_{K_P-1}}\right\}, \tag{14}$$

$$\dot{\varphi}_T[t_P] = \left\{t_{P_0} : \dot{\varphi}_{T_0}, t_{P_1} : \dot{\varphi}_{T_1}, ..., t_{P_{K_P-1}} : \dot{\varphi}_{T_{K_P-1}}\right\}, \tag{15}$$

where K_P is simply the total number of samples available.[6] On the spacecraft, a phase measurement of the received uplink signal is captured every time a frame departs. This yields a discrete-time series

$$\varphi_S[t_S] = \left\{ t_{S_0} : \varphi_{S_0}, t_{S_1} : \varphi_{S_1}, ..., t_{R_{K_S-1}} : \varphi_{T_{K_S-1}} \right\}, \tag{16}$$

where K_S is the number of samples. However, only the samples φ_{S_i} are sent to the ground and arrive to the ground station at t_{R_i}.[7] This results in another discrete-time series

$$\varphi_S[t_R] = \left\{ t_{R_0} : \varphi_{S_0}, t_{R_1} : \varphi_{S_1}, ..., t_{R_{K_R-1}} : \varphi_{T_{K_R-1}} \right\}, \tag{17}$$

where K_R is the number of samples available and we have implicitly associated a sample measured on board the spacecraft with its time of arrival on the ground. Note that, in general, $K_R = K_S$ but $K_R \neq K_p$. Indeed, the time series $\varphi_T[t_P]$ and $\varphi_S[t_R]$ are sampled by completely unrelated events triggered at potentially different rates.

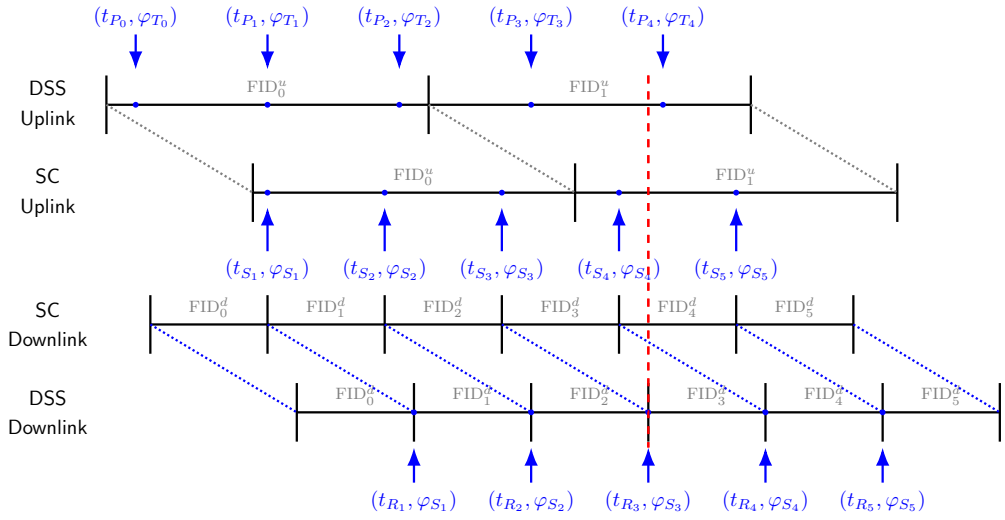

Figure 4. Discrete-Time Measurements

Let us now assume that range measurements at time t_R are to be recovered (recall here that we have chosen t_R to denote an instant in time that coincides with the arrival of a downlink frame). Then, we first need to infer all parameters required to solve Equation (8). In particular,

- t_R is a known input.

---

[6] By convention, we denote all continuous signals as $x(t)$ and use $x[t_i], i \in [0, K]$ for their discrete counterpart. In this notation, K is simply the total number of samples available in the measured dataset.

[7] In reality, the instants of time t_{R_i} might be reconstructed after the fact through digital processing from high-rate samples of an open-loop recording, a consideration obviated in this document for simplicity.

- t_T is the unknown output that we wish to estimate.
- $\varphi_T(t)$ and $\dot{\varphi}_T(t)$ are available as a set of discrete samples $\dot{\varphi}_T[t_P]$ and $\dot{\varphi}_T[t_P]$. If higher sampling rate is required, then additional samples are obtained via interpolation.
- $\varphi_T(t_T)$ is not directly available. However, by virtue of Equation (9) it is equal to $\varphi_S(t_S)$ and therefore we can use the received samples $\varphi_S[t_R]$.

Therefore, in the discrete domain Equation (8) becomes

$$\sum_{t_T}^{t_x} \dot{\tilde{\varphi}}_T[t] = \varphi_R[t_x] - \varphi_S[t_R]. \tag{18}$$

Here, we use the tilde operator to emphasize the fact that increased precision in solving Equation (8) might require interpolation. We have also substituted the continuous-time integral by a discrete-time summation and referenced the second term of the equation's right-hand side to t_R to emphasize that the phase sample taken on board the spacecraft at t_S is received on the ground at time t_R.

1. Additional Considerations

Up until this point, we have made two implicit simplifying assumptions to facilitate the discussion. First, we have referenced all range calculations to t_R, an instant of time associated with the start of arrival of a downlink frame at the ground station. And secondly, we have assumed that a phase measured on board the spacecraft can be encoded as part of the payload of the downlink frame that triggered it. We now show that both assumptions are not necessary for the system to work and propose alternatives that are easier to implement.

Let us first consider the time at which a range measurement is to be taken. Up until now, we have assumed that this happens at t_R, an instant in time that corresponds to the arrival of downlink frame from the spacecraft. In reality, however, receivers do not usually have the ability to detect the start of an arriving frame. Instead, they rely on synchronization markers[8] that are included as part of the framing structure. Therefore, instead of associating t_R with the arrival of a frame, it is generally preferable to associate it with the detection of a synchronization marker. Note that this introduces an offset to the entire measurement system. However, since this offset is the same for both terms of the right side of Equation (8), they cancel each other out, thus no modification to the system is needed.

On the other hand, we have also assumed that any phase measurement φ_{S_i} on board the spacecraft can be encoded as part of the payload of the frame that triggered it.

---

[8]The exact hexadecimal value of these markers typically can be found in communication standards.

Mathematically, this results in a time series of samples, at the receiver,

$$\varphi_S[t_R] = \{t_{R_i} : \varphi_{S_i}\}, i \in [0, K_R - 1]. \tag{19}$$

However, a frame departing the spacecraft is generally fully formed and no new information can be appended to it. Therefore, the ith measurement φ_{S_i} will have to be telemetered back to Earth as part of a later frame, leading to received samples of the form

$$\varphi_S[t_R] = \left\{t_{R_j} : \varphi_{S_i}\right\}, j > i,\ i \in [0, K_R - 1]. \tag{20}$$

Consequently, we need a mechanism to associate samples arriving at the ground station with the downlink frame that triggered latching on board the spacecraft. For instance, a simple approach is to explicitly transmit the identifier of this frame together with phase measurement. In other words, the jth frame will contain the tuple $\left(\varphi_{S_i}, \mathrm{FID}_i^d\right)$ and, upon receipt at the ground station, the measurement φ_{S_i} will be associated with the instant in time t_{R_i} corresponding to the arrival of the ith frame.

2. Phase Measurement Specification

We now consider how samples of $\varphi(t)$ (either at the spacecraft or ground station) can be constructed from elements measurable in a space optical communication system. To facilitate the discussion, Figure 5 shows a notional timeline in which frames arrive to the spacecraft at a cadence of $1/T_f$ Hz. Each frame carries a unique FID that is encoded in the frame header using a certain number of bits, giving rise to a counter that periodically resets (in Figure 5, for simplicity, we assumed that only 2 bits are available). Also, each frame lasts for 14 slots (see blue plot), an unrealistically low value chosen for clarity.

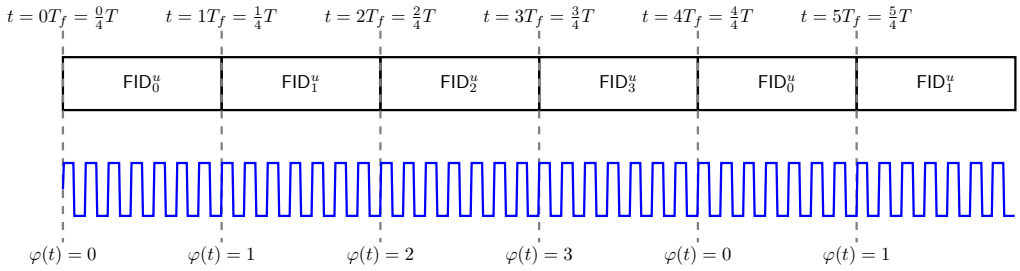

Figure 5. Phase Specification

In the system shown in Figure 5, the ground station sends frames to a single spacecraft. At the receiving end, its radio makes four measurements:

1. It records the frame ID of the uplink frame currently being processed as a tuple of identifiers (e.g., spacecraft ID, virtual channel ID, virtual channel counter). This value, denoted by FID^u, is encoded as a fixed-size bit pattern of length n_{fu}.

2. It recovers the slot clock from the uplink signal and uses it to count how many slots have elapsed since the frame's synchronization marker. This value, denoted by s, ranges from 0 to $N_s - 1$ and is encoded using n_s bits (i.e., N_s denotes the total number of slots that elapse per uplink frame).

3. It uses the receiver's slot tracking loop to determine, at any given point in time, the fraction of slot elapsed since the last slot ended. This value, denoted by ϵ, ranges from 0 to 1 and is encoded using n_ϵ bits.

4. It records the frame ID of the downlink frame that triggered the latching mechanism to measure items (1) through (3). This value, denoted by FID^d is encoded as a fixed-size bit pattern of length n_{fd}.

These four values, occupying a total of $n = n_{fu} + n_s + n_\epsilon + n_{fd}$ bits, are then placed as part of the payload bits of a telemetry frame and sent to the ground. Once there, these n bits are separated from the rest of telemetry stream and routed to the ranging post-processing system.

Let $\boldsymbol{\Phi}_j$ denote the four-element tuple measured on board the spacecraft and conveyed to the ground by the jth frame of the downlink stream. Furthermore, let t_{R_j} denote the time of arrival of that frame, and let FID_j^d denote its identifier. Then, the normalized and unwrapped phase measurement to be used for ranging can be recovered as follows:

1. Decode the different parts of $\boldsymbol{\Phi}_j$ to recover FID_i^u, s_i, ϵ_i, and FID_d^i. Note that in general $i < j$ based on the discussion from the previous section.

2. Infer the time of arrival of the ith downlink frame, whose departure triggered the phase measurement on board the spacecraft. This instant of time, denoted t_{R_i}, will provide a time tag for the rest of the range computation.

3. Obtain a zero-based numerical index $\alpha_i \in \mathbb{N}$ that identifies the relative position of the uplink frame identified by FID_i^u within the uplink stream sent by the ground station. This can be easily performed if the station records the order in which frames depart towards the spacecraft.

4. Add s_i and ϵ_i and then normalize by N_s, the total number of slots elapsed by uplink frame, a value assumed constant and known a priori.

5. Recover the $\varphi_S[t_{R_i}]$ as

$$\varphi_S[t_{R_i}] = \alpha_i + \frac{s_i + \epsilon_i}{N_s}. \tag{21}$$

This procedure is then repeated for each ranging sample arriving at the ground station through the telemetry stream, thus resulting in the set $\varphi_S[t_R]$.

C. OTR Phase Encoding

We now consider how a measured phase sample $\boldsymbol{\Phi}$ should be encoded as part of the telemetry stream. To ground the analysis on realistic systems, we assume that the proposed optical ranging system should be compatible with CCSDS optical standards, namely the Optical Communications Physical Layer [12] and Coding and Synchronization Layer [13]. Additionally, we also consider compatibility with the CCSDS optical on-off keying (O3K) standard that is currently under development.

Current CCSDS optical standards assume that PPM is used to encode bits onto the optical signal (for the purposes of this article, O3K can be viewed as 2-PPM). They define a wide variety of slot widths, PPM orders and coding rates which, together, allow system designers to vary the link data rate over several orders of magnitude. This, in turn, allows the standard to be compatible over a wide range of link conditions and distances. For instance, Table 1 lists the modes of operation of JPL's Deep Space Optical Communications (DSOC) terminal to be tested on board the Psyche spacecraft. Note that the link data rate can vary from 260 Mbps to just 56 kbps, a difference in data rate of almost five orders of magnitude.

Table 1. DSOC Operational Modes

PPM Order	Code Rate	Symbol Repeat	Slot Width [ns]	Data Rate [Mbps]	Frame [msec]	Num. slots per frame
16	2/3	1	0.5	264.65	0.03	67,411
16	2/3	1	1	123.32	0.07	67,411
32	1/3	1	0.5	82.34	0.11	216,674
32	1/3	1	1	41.17	0.22	216,674
64	1/3	1	1	24.68	0.36	361,504
128	2/3	1	2	14.43	0.62	309,137
128	1/3	1	2	7.19	1.24	620,373
128	1/2	1	4	5.40	1.65	1,861,119
128	1/3	1	4	3.60	2.48	620,373
128	1/3	3	2	2.40	3.72	1,861,119
128	1/3	1	8	1.80	4.96	620,373
128	1/3	2	8	0.90	9.93	1,240,746
128	1/3	8	8	0.23	39.70	4,962,984
128	1/3	32	8	0.06	158.82	19,851,936

Let us now consider that OTR was being designed as part of the DSOC communications payload and assume that all DSOC transfer frames have a constant duration of 8920 bits. Table 1 shows the total number of slots N_f that elapse per frame for each of the available operational modes. Observe that this value varies over three orders of magnitude. Practically, this means that the number of bits required to encode N_f varies from 17 bits in the first mode of operations, to 25 bits in the last

one. Therefore, in Sections III.C.1 and III.C.2 we explore how $\boldsymbol{\Phi}$ should be represented in binary format using variable vs. fixed-length encoding. Evidently, the variable-length encoding is more bandwidth efficient, but it also leads to increased decoding complexity and processing time.

1. Variable-Length Encoding

First, let us consider how to encode the ID of the uplink and downlink frames. The CCSDS optical communication standards assume that the framing structure is inherited from data link layer protocols used in RF communications, namely the Advanced Orbiting Systems (AOS) Space Data Link Protocol [14], the Telemetry (TM) Space Data Link Protocol [15], and the Unified Space Data Link Protocol (USLP) [16]. Frames are consequently uniquely identified through a tuple of values that depend on the protocol data unit structure:

- AOS Protocol: Transfer Frame Version Number (2 bits), Spacecraft ID (8 bits), Virtual Channel ID (6 bits), Virtual Channel Frame Count (24 bits), for a total of 40 bits.
- TM Protocol: Transfer Frame Version Number (2 bits), Spacecraft ID (10 bits), Virtual Channel ID (3 bits), Master Channel Frame Count (8 bits), Virtual Channel Frame Count (8 bits), for a total of 31 bits.
- USLP Protocol: Transfer Frame Version Number (4 bits), Spacecraft ID (16 bits), Virtual Channel ID (6 bits), MAP ID (4 bits), Virtual Channel Frame Count Length (3 bits), Virtual Channel Frame Count (0 to 56 bits, variable), for a total of 33 to 92 bits.

Therefore, an absolute minimum of 62 bits and an absolute maximum of 184 bits will be required to encode FID^u and FID^d depending on which protocols are used on the uplink and downlink. Note that this range of bits does not depend on the link mode of operations. Indeed, missions like DSOC typically choose a data link layer protocol during their design phase and it remains unchanged for the rest of the mission.

Next, we consider the number of bits required to encode the integer number of slots elapsed since the frame's synchronization marker, s, a value that can be simply estimated as $n_s = \lceil \log_2 N_f \rceil$, where N_f is the number of slots that can possibly elapse during a single frame. Using the values from Table 1, we get that $n_s \in [17, 25]$ bits, depending on the mode of operations. Finally, we consider the number of bits to encode ϵ. In that sense, RF ranging standards have typically assumed a desired ranging resolution of $RR = 1$ ps. Therefore, and given a slot duration of T_s seconds, the number of bits required to encode n_ϵ can be estimated as

$$n_\epsilon = \left\lceil \log_2 \frac{T_s}{RR} \right\rceil. \tag{22}$$

In the case of DSOC, the slot duration varies between 0.5 and 8 ns, which results in $n_\epsilon \in [9, 13]$ bits. In other words, we have reached the conclusion that for DSOC, $\boldsymbol{\Phi}$ can be encoded using $n \in [106, 114]$ bits depending on which data link layer protocol and link mode are chosen.[9] Note that, in reality, some additional overhead will be needed to delimit the different parts of the four-element tuple $\boldsymbol{\Phi}$. However, we obviate this consideration for simplicity.

Finally, Table 2 helps illustrate a general characteristic of how phase measurements will be encoded in OTR systems. In particular, it can be observed that the majority of bits used are allocated for encoding FID^u and FID^d, both of which are fixed in size and do not depend on the link mode. Consequently, this leads to the conclusion that bandwidth savings from variable-length encoding are likely to be small and not worth the additional complexity they entail.

Table 2. Variable Phase Encoding for DSOC

PPM Order	Code Rate	Symbol Repeat	Pulse Width [ns]	Data Rate [Mbps]	Encoding Bits				
					n_ϵ	n_s	n_{fu}	n_{fd}	n
16	2/3	1	0.5	263.59	9	17	40	40	106
16	2/3	1	1	131.80	10	17	40	40	106
32	1/3	1	0.5	82.29	9	18	40	40	107
32	1/3	1	1	41.14	10	18	40	40	107
64	1/3	1	1	24.66	10	19	40	40	108
128	2/3	1	2	14.37	11	19	40	40	108
128	1/3	1	2	7.18	11	20	40	40	109
128	1/2	1	4	5.39	12	19	40	40	108
128	1/3	1	4	3.59	12	20	40	40	109
128	1/3	3	2	2.39	11	21	40	40	110
128	1/3	1	8	1.80	13	20	40	40	109
128	1/3	2	8	0.90	13	21	40	40	110
128	1/3	8	8	0.22	13	23	40	40	112
128	1/3	32	8	0.06	13	25	40	40	114

2. Fixed-Length Encoding

Fixed-length encoding systems are significantly simpler to implement. In this case,

- FID^u and FID^d are encoded as before and therefore require the same number of bits.
- s needs to be sized so that, in the worst possible case, the desired range ambiguity can be resolved within a single uplink frame. For instance, RF ranging

[9] A similar calculation can be performed over all modes supported by the CCSDS optical standards to show that the absolute minimum and maximum values of n are 87 and 225, respectively.

standards typically set RA= 0.5 seconds. Therefore, if the upcoming O3K optical standard defines a minimum slot size of 0.1 ns, then $n_s = \lceil \log_2 \frac{0.5s}{0.1ns} \rceil = 33$ bits.

- Also, given a desired range resolution of 1 ps and a maximum slot width of 65,536 ns (see Reference [12]), in the worst case, $n_\epsilon = 26$ bits.

Combining these values leads to the conclusion that fixed-length encoding will require a total of $n \in [121, 243]$ bits, compared to $n \in [87, 225]$ bits in variable-length encoding. This additional overhead, however, does not lead to significant bandwidth inefficiency. To exemplify this, Table 3 calculates this figure-of-merit assuming that the OTR phase measurements are encoded using a fixed-length 256-bit field[10] and four modes of operation are allowed: modes 1 and 4 are stretch cases that represent the maximum and minimum data rate allowed by the CCSDS optical standards; and modes 2 and 3 are based on DSOC. Observe that the information rate (which is defined as the data rate, net of ranging bits) varies between 2.1 Gbps and 420 bps. Only the latter case, which is the absolute minimum data rate supported by the standard, exhibits high bandwidth overhead. However, it can be argued that a link

Table 3. Bandwidth Efficiency for CCSDS HPE Telemetry Links

	Mode 1	**Mode 2**	**Mode 3**	**Mode 4**
Inputs				
Frame Size [bits]	65536	8920	8920	1024
PPM Order	4	16	128	256
Slot Width [nsec]	0.125	0.5	4	512
Code Rate	2/3	2/3	1/2	1/3
Symbol Repeat	1	1	1	32
Data Rate				
CSM length [PPM symbols]	24	16	16	16
PPM Symbols per codeword	7560	3780	2160	1890
Data Rate [Mbps]	2119.41	264.65	5.40	0.0005
Measurement Frequency				
Min [Hz]	0.01	0.01	0.01	0.01
Typical [Hz]	0.1	0.1	0.1	0.1
Max [Hz]	1	1	1	1
Information Rate				
Min [Mbit/s]	2119.41	264.65	5.40	0.0005
Typical [Mbps]	2119.41	264.65	5.40	0.0005
Max [Mbps]	2119.41	264.65	5.40	0.0002
Bandwidth Efficiency [%]				
Min	99.999	99.999	99.999	99.488
Typical	99.999	99.999	99.999	94.889
Max	99.999	99.999	99.995	48.897

[10] 256 bits are chosen so that the size of the bit-field is a multiple of an octet.

operating at this rate should either not perform ranging at the same time, or the measurement cadence should be reduced to 0.1 Hz to increase the bandwidth efficiency to approximately 95%.

IV. OTR Functional Architecture

We now provide a brief description of the signal processing blocks that need to be implemented to obtain ranging measurements from an OTR system. In particular, we provide functional block diagrams for four elements: the ground station uplink transmitter, the spacecraft uplink receiver, the spacecraft downlink transmitter, and the ground station downlink receiver. Also, through the rest of the document, all functional blocks are color-coded according to the following convention:

- Black blocks are tasked with taking information bits as input and transforming them into a sequence of slots to be transmitted by the optical laser (and vice-versa).
- Gray blocks represent all analog functionality. For simplicity purposes, they are simply encapsulated as a laser that shifts the transmitted signal from the baseband domain to the desired optical frequency.
- Orange blocks provide timing signals. They are typically driven by an oscillator at the slot frequency, which is then divided appropriately to provide synchronous slot, symbol, and frame processing.
- Blue blocks are related to the OTR ranging mechanism, most notably measurement of the transmitted and received phases.
- Red blocks are inputs to a subsystem.
- Green blocks are outputs of a given subsystem. The final range measurement is considered as an output of the ground station's downlink processing (see Figure 9), although this need not be the case in a real implementation.

A. Uplink Signal Processing at the Ground Station

Figure 6 provides a high-level overview of the ground station uplink transmit functionality assuming an M-PPM modulation is used. This is presented for the purpose of concreteness, and a similar system would work with O3K or RF uplink transmissions. Next, we describe the different parts of Figure 6 focusing mainly on their relevance to the ranging system.

First, commanding data is encapsulated into AOS, TM, or ULSP frames by the Uplink Frame Generator (UFG). If no commanding data is available, then fill data in the form of alternating logical 0s and 1s is presented to the UFG for processing. Also,

while creating a frame, the UFG prepends a header that includes the identifier described in Section III.C.1 and denoted as FID^u.

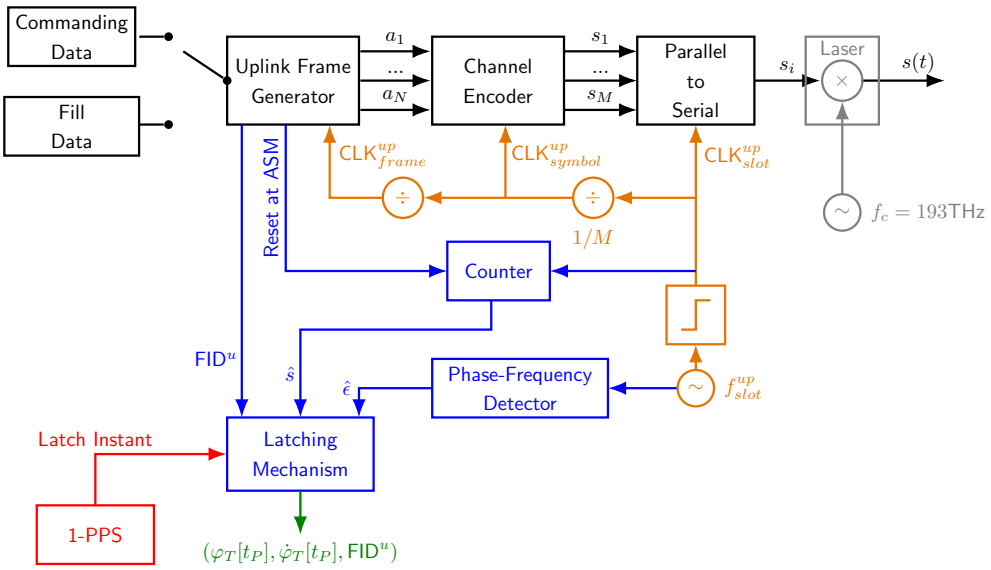

Figure 6. Ground Station Uplink Transmitter

Once the uplink frame is generated, it is passed onto a processing block that performs coding and synchronization functionality in accordance to the Optical Coding and Synchronization standard [13]. In that sense, the first step is to append an Attached Synchronization Marker (ASM) to the transfer frame to produce a Synchronization-Marked Transfer Frame (SMTF). This ASM is a standardized hexadecimal sequence that is known by the transmitter and receiver and can therefore be used to separate contiguous transfer frames in a continuous data stream.

Next, the SMTF undergoes several operations to transform its logical bits into a series of modulated symbols. These include slicing, coding, and interleaving, among others. At the end of this process, a set of modulated symbols are available, each one containing of M slots $\{s_1, ..., s_M\}$.[11] Finally, each slot s_i is transformed into a light pulse using a high-power laser, which yields the transmitted optical signal $s(t)$.

The data processing steps previously described are typically driven by a common reference clock that is derived from a highly-stable oscillator running at the desired slot rate f_{slot}. This clock is divided by M and N_f to infer the instants in time when new PPM symbols and frames are ready for further processing.[12] This ensures that

[11] This notation is adapted from the CCSDS optical coding and synchronization standard and is particularly well suited for M-PPM. For O3K and DPSK modulations, simply assume that $M = 1$.

[12] In reality, each PPM symbol requires a certain guard time, a consideration that has been obviated in these diagrams for simplicity. As an example, the CCSDS HPE telemetry standard uses $\frac{5}{4}M$ slots per

the entire processing block in the transmitter is synchronized and prevents buffer overflows at the input/output of each processing block.

Finally, ranging measurements are obtained via a latching mechanism that requests the value of FID^u, s, and ϵ whenever an external event is triggered by the ground station 1-PPS clock. In particular, FID^u is generally read directly from the internal register in the UFG, s is obtained from a counter that is incremented by the slot clock and that resets at the ASM of each departing frame, and ϵ is obtained through a phase-frequency detector connected to the station's slot clock.

B. Uplink Signal Processing at the Spacecraft

Figure 7 shows the main functional blocks of the spacecraft receiver. The received signal is first transformed from the optical domain to an electric voltage via a light detector, a signal that drives a time-to-digital converter that records the arrival of every light photon. This sequence of time tags is then routed to a slot synchronizer that, internally, uses a slot timing recovery algorithm to recover the slot clock from the received signal. Furthermore, as indicated in Reference [9], this algorithm also produces an estimate of ϵ, the fractional phase measurement of the OTR's ranging procedure.

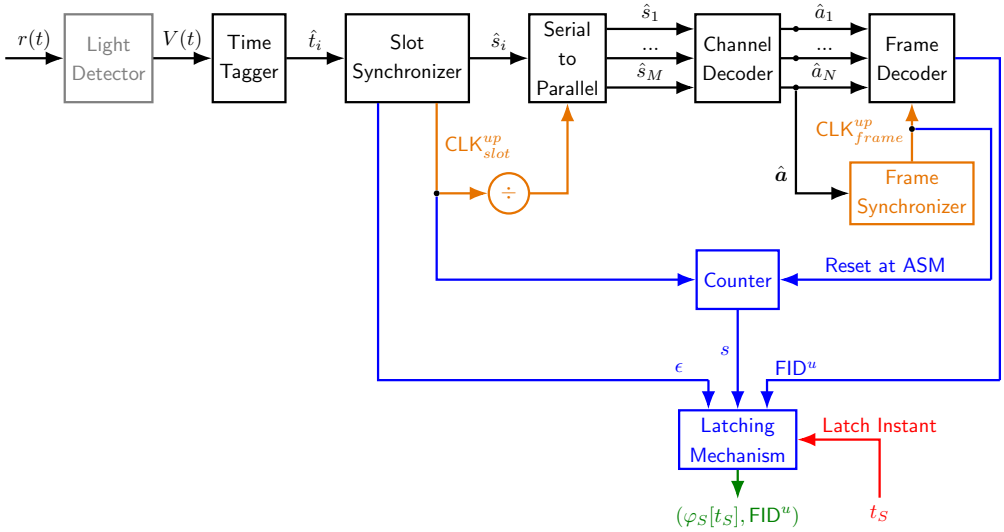

Figure 7. Spacecraft Uplink Receiver

Once the slot clock has been recovered, then the rest of the data processing chain can be synchronized to that clock. This ensures that sequential processing occurs even in the presence of Doppler effects that shorten/lengthen the duration of each slot and thus change the effective slot rate. As for ranging, an estimate of s can simply be

---

PPM symbol.

obtained with a counting device that increases an internal registry at the rising edge of the slot clock. Similar to the ground station transmitter, this counter is reset every time that a frame ASM is detected, an event that is provided by the frame synchronizer. Finally, a phase measurement $(\text{FID}^u, s, \epsilon)$ is recorded every time an external signal triggers the latching mechanism, an event that we denote by t_S and is explained in the next section.

C. Downlink Transmit Processing

Figure 8 shows the functional diagram of the spacecraft's downlink transmit functionality. From a data processing standpoint, most of the system is analogous to the blocks shown in Figure 6 since transfer frames have to be turned into a sequence of slots that can be modulated by a laser to the optical carrier. From a timing standpoint, note that the transmitter is driven by a local oscillator at the downlink slot rate, which is not related in any manner to the recovered slot clock in the spacecraft's uplink subsystem. This ensures that the spacecraft's uplink and downlink subsystem are fully asynchronous and allows the uplink and downlink to operate at different PPM modes (and therefore at different data rates).

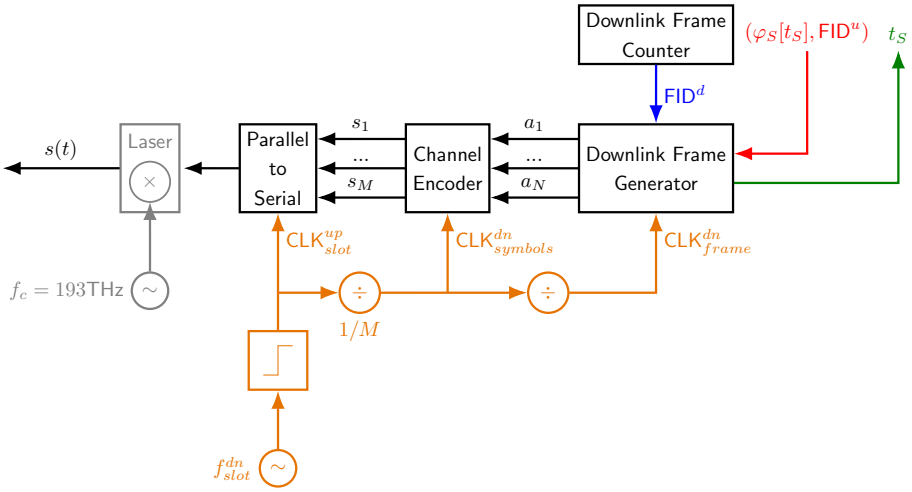

Figure 8. Spacecraft Downlink Transmitter

On the other hand, there are only two parts of the spacecraft downlink subsystem that are relevant to OTR. First, OTR requires a downlink frame counter that updates the value of the FID^d every time a downlink frame departs. This information, together with the uplink phase measurement $\varphi_S[t_S]$, are combined to form $\boldsymbol{\Phi}$, the tuple that will be sent to the ground for further processing.[13] Second, the downlink frame generator provides a signal to the spacecraft's uplink subsystem every time a phase

[13]Note that $\boldsymbol{\Phi}$ might be placed in the next frame departing, or might be stored on board the spacecraft and returned at the end of the pass, a possibility not shown in Figure 8 for simplicity.

measurement needs to be acquired. This can coincide, for instance, with the rising edge of an ASM at the output of the frame generator. Other triggers are also possible as long as the ground station uses a consistent trigger to time-tag the arrival of $\boldsymbol{\Phi}$.

D. Downlink Receive Processing

Figure 9 depicts the set of blocks required to implement the optical ranging system at the grounds station's receiver. In particular, we assume that the ground telescope is equipped with a photon-counting device that time-tags the arrival of each photon. This information is routed to a slot synchronizer that recovers the downlink slot clock and outputs slot values to a serial-to-parallel converter. Once M slots are recovered, then they are passed as a symbol to the next functional block to generate codeblocks and, eventually, to recover entire transfer frames.

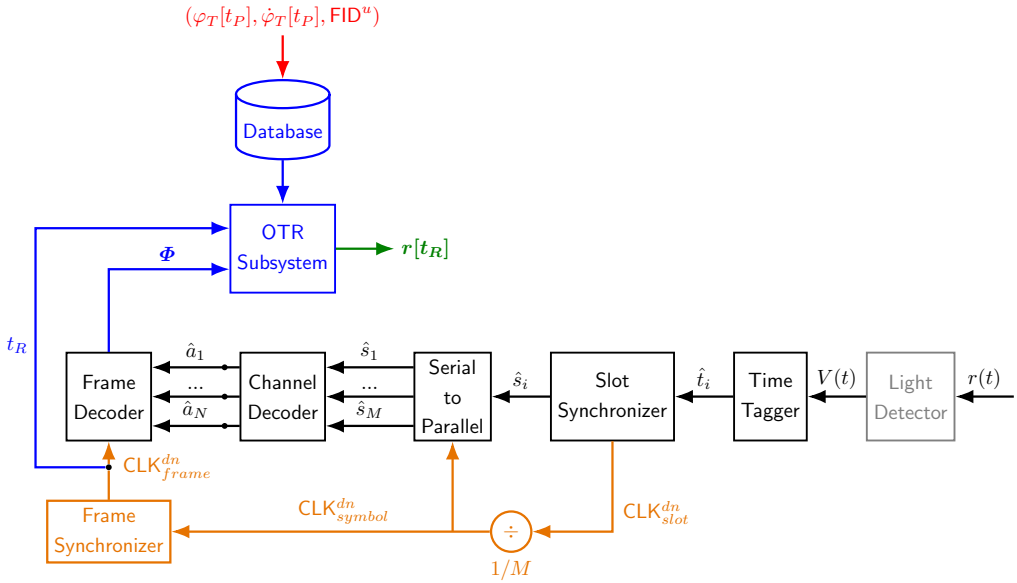

Figure 9. Ground Station Downlink Receiver

Once a transfer frame has been recovered, the range measurement $\boldsymbol{\Phi}$ encoded as part of its payload is extracted and delivered to the OTR subsystem together with a time tag that indicates the instant in time associated with $\boldsymbol{\Phi}$. This OTR subsystem can be implemented to obtain range estimates in real-time (which most likely requires a hardware implementation to handle the large sample rates of typical optical links) or, alternatively, can be used to deliver ranging products sometime after the pass has ended (in which case a software implementation suffices). In either case, however, the OTR subsystem pulls information from a database that contains the phase measurements taken by the ground station's uplink subsystem and combines them with $\boldsymbol{\Phi}$ using the procedure detailed in Section III.B to obtain the final range estimates $r[t_R]$.

V. Conclusions

The concept of Optical Telemetry Ranging is an adaptation of RF Telemetry Ranging for space-to-ground links operating at optical frequencies. At its core, OTR embraces the philosophy of not requiring the spacecraft to echo back the ranging signal to the ground station. Instead, phase measurements required for estimating range are conducted on board the spacecraft and then telemetered back to Earth for further processing. This reduces the power required to conduct ranging and, more importantly, eliminates the need for dedicated ranging passes.

To explain how OTR works, this article initially considers an idealized setup in which all signals are continuous and measurements can be performed instantaneously. In that case, we show that range estimates can be recovered by integrating the transmitted Doppler frequency, a process that has been the basis for ranging since the early days of spaceflight. We present how the same result can be achieved in a realistic discrete-time system where transmitter and receiver are driven by clocks that are not synchronous. We then detail how phase measurements on board the spacecraft should be encoded to be compatible with current optical standards. This, in turn, allows us to demonstrate that OTR has minimal bandwidth overhead on the telemetry stream.

Several avenues for future work have been identified while writing this article. For instance, the performance of OTR should be evaluated for current and planned optical missions, including DSOC and the Optical-to-Orion (O2O) system. In that sense, ranging uncertainty as a function of distance, PPM mode, and Sun-Probe-Earth angle, should be quantified and reported in a future article. On the other hand, technical investments to incorporate OTR capabilities on JPL's optical ground receivers should also be considered. This includes, for instance, implementation of OTR or alternative ranging techniques in the optical receivers at JPL's Table Mountain Facility (TMF) in Wrightwood, CA.

References

[1] Jet Propulsion Laboratory, "Sequential Ranging," Jet Propulsion Laboratory, Tech. Rep. 810-005, 203, Rev. D, June 2019.

[2] Consultative Committee for Space Data Systems, "Pseudo-Noise (PN) Ranging Systems," Consultative Committee for Space Data Systems, Tech. Rep. CCSDS 414.1-B-2, February 2014.

[3] ——, "Pseudo-Noise (PN) Ranging Systems," Consultative Committee for Space Data Systems, Tech. Rep. CCSDS 414.0-G-1, February 2014.

[4] ——, "Simultaneous Transmission of GMSK Telemetry and PN Ranging," Consultative Committee for Space Data Systems, Tech. Rep. CCSDS 413.1-G-1, May 2017.

[5] ——, "Radio Frequency and Modulation Systems: Part 1. Earth Stations and Spacecraft," Consultative Committee for Space Data Systems, Tech. Rep. CCSDS 401.0-B-30, February 2020.

[6] G. W. Heckler, A. Long, L. M. Winternitz, J. Donaldson, and G. Yang, "Metric Tracking Services in the Era of Optical Communications," 70th International Astronautical Congress (IAC), Washington D.C., October 21–25 2019.

[7] M. Stevens, R. Parenti, M. Willis, J. Greco, F. Khatri, B. Robinson, and D. Boroson, "The Lunar Laser Communication Demonstration Time-of-Flight Measurement System: Overview, On-orbit Performance, and Ranging Analysis," in *Free-space Laser Communication and Atmospheric Propagation XXVIII*, vol. 9739, International Society for Optics and Photonics, 2016, p. 973908.

[8] J. Hamkins, P. Kinman, H. Xie, V. Vilnrotter, and S. Dolinar, "Telemetry Ranging: Concepts," *The Interplanetary Network Progress Report*, vol. 42-203, Jet Propulsion Laboratory, Pasadena, California, pp. 1–20, November 15 2015. https://ipnpr.jpl.nasa.gov/progress_report/42-203/203C.pdf

[9] ——, "Telemetry Ranging: Signal Processing," *The Interplanetary Network Progress Report*, vol. 42-204, Jet Propulsion Laboratory, Pasadena, California, pp. 1–56, February 15 2016. https://ipnpr.jpl.nasa.gov/progress_report/42-204/204D.pdf

[10] J. Hamkins, P. Kinman, H. Xie, V. Vilnrotter, S. Dolinar, N. Adams, E. Sanchez, and W. Millard, "Telemetry Ranging: Laboratory Validation Tests and End-to-End Performance," *The Interplanetary Network Progress Report*, vol. 42-206, Jet Propulsion Laboratory, Pasadena, California, pp. 1–35, August 15 2016. https://ipnpr.jpl.nasa.gov/progress_report/42-206/206D.pdf

[11] Goddard Space Flight Center, "The Doppler Equation in Range and Range Rate Measurements," NASA, Tech. Rep. X-507-65-385, October 1965. https://ntrs.nasa.gov/archive/nasa/casi.ntrs.nasa.gov/19660010159.pdf

[12] Consultative Committee for Space Data Systems, "Optical Communications Physical Layer," Consultative Committee for Space Data Systems, Tech. Rep. CCSDS 141.0-B-1, August 2019.

[13] ——, "Optical Communications Coding and Synchronization," Consultative Committee for Space Data Systems, Tech. Rep. CCSDS 142.0-B-1, August 2019.

[14] ——, "AOS Space Data Link Protocol," Consultative Committee for Space Data Systems, Tech. Rep. CCSDS 732.0-B-3, September 2015.

[15] ——, "TM Space Data Link Protocol," Consultative Committee for Space Data Systems, Tech. Rep. CCSDS 132.0-B-2, September 2015.

[16] ——, "Unified Space Data Link Protocol," Consultative Committee for Space Data Systems, Tech. Rep. CCSDS 732.1-B-1, October 2018.